

Article

Evolutionary Algorithm to Optimize Process Parameters of Al/Steel Magnetic Pulse Welding

Jiyeon Shim ¹  and Illsoo Kim ^{2,*}

¹ Carbon & Light Materials Application R&D Group, Korea Institute of Industrial Technology, Jeonju-si 54853, Republic of Korea; shimjy@kitech.re.kr

² Department of Mechanical Engineering, Mokpo National University, 1666 Youngsan-ro, Chungkye-myun, Muan-gun 58554, Republic of Korea

* Correspondence: ilsookim@mokpo.ac.kr

Abstract: The Magnetic Pulse Welding (MPW) process uses only electromagnetic force to create a solid-state metallurgical bond between a working coil and outer workpiece. The electromagnetic force drives the outer tube to collide with the inner rod, resulting in successful bonding. However, due to the dissimilarity of the MPW joint, only a portion of the interface forms a metallurgical bond, which affects the quality of the joint. Therefore, the purpose of this study is to analyze the effects of process parameters on joint quality through experimental work using RSM. Furthermore, an optimization algorithm is utilized to optimize the process parameters used in magnetic pulse welding. A1070 aluminum and S45C carbon steel were used as the materials, while peak current, gap between working coil and outer tube, and frequency were chosen as the process parameters for MPW. The welding conditions are determined through experimental design. After welding, the maximum load and weld length are measured to analyze the effect of the process parameters, and a prediction model is developed. Specifically, to achieve a high-quality joint, the process parameters are optimized using the Imperialist Competitive Algorithm (ICA) and Genetic Algorithm (GA). The results reveal that the peak current is a significant parameter, and the developed prediction model exhibits high accuracy. Furthermore, the ICA algorithm proves very effective in determining the process parameters for achieving a high-quality Al/Steel MPW joint.



Citation: Shim, J.; Kim, I. Evolutionary Algorithm to Optimize Process Parameters of Al/Steel Magnetic Pulse Welding. *Appl. Sci.* **2023**, *13*, 12881. <https://doi.org/10.3390/app132312881>

Academic Editors: Ivan Galvão, Rui Manuel Leal and Gustavo H. S. F. L. Carvalho

Received: 31 October 2023
Revised: 20 November 2023
Accepted: 25 November 2023
Published: 30 November 2023



Copyright: © 2023 by the authors. Licensee MDPI, Basel, Switzerland. This article is an open access article distributed under the terms and conditions of the Creative Commons Attribution (CC BY) license (<https://creativecommons.org/licenses/by/4.0/>).

Keywords: magnetic pulse welding; evolutionary algorithm; electromagnetic force; process parameters; Imperialist Competitive Algorithm; Genetic Algorithm

1. Introduction

In the field of automotive engineering, a main challenge facing automakers is to reduce harmful greenhouse gas emissions by decreasing fuel consumption [1,2]. One effective solution for this is to decrease the weight of automotive body assemblies. However, it is crucial to ensure that any weight reduction in the body assembly does not compromise passenger safety. Therefore, lightweight materials with high strength, such as aluminum and magnesium, have been implemented in automotive body construction. Nonetheless, the use of only lightweight materials may mean that specific components do not meet required specifications, so there is a need to develop integration processes for dissimilar materials.

Certain welding processes have been considered for integrating dissimilar materials. Fusion welding methods, such as conventional welding, laser beam welding, and resistance welding, have been studied. Zhao et al. [3] and Chen et al. [4] aimed to enhance the synergy between strength and ductility while also improving the corrosion resistance of a dissimilar joint between Inconel 718 and 316L. Pan et al. [5] conducted a study on the formation mechanisms of intermetallic compounds in a dissimilar joint between aluminum and steel. This investigation was carried out using resistance spot welding. However, the high heat input in these fusion welding processes caused not only thick intermetallic

compound (IMC) layers between materials but also cracking, porosity, and oxidation [5]. For this reason, friction stir welding, explosive welding, and magnetic pulse welding have recently been widely studied as methods of solid-state welding. Yang et al. [6] conducted a numerical analysis to investigate the process of mass transfer and material mixing in friction stir welding of dissimilar joints. Bhattacharya et al. [7] attempted to join aluminum alloy to DHP copper using friction stir welding. This process has the capability to produce high-quality joints between different combinations of materials. However, due to tool conditions, several types of defects may occur in joints, such as thickness reduction and flash and keyhole defects [8]. Explosive welding utilizes explosive force to create a successful metallurgical bond between workpieces. Kumar et al. [9] reported on the welding of magnesium and aluminum alloys using an inclined arrangement in explosive welding, while Carvalho et al. [10] studied the effect of flyer material on interface phenomena in explosive welds of aluminum and copper. However, controlling the process parameters is difficult, and experimental work can be unsafe. For this reason, Magnetic Pulse Welding (MPW), a solid-state welding process, has been used in the development of high-quality dissimilar joints. MPW is a high-velocity welding process using an electromagnetic force to cause high-velocity collisions between dissimilar materials, resulting in true metallurgical bonds. MPW uses only electromagnetic force, without filler wire, as shown in Figure 1. It is an environmentally friendly welding process [11,12]. When using MPW for the welding of dissimilar materials such as aluminum and steel, a challenge for researchers is selecting the proper welding parameters to create strong joints with excellent properties. The main process parameters of MPW, including input current, gap between workpieces, and frequency, play important roles in determining joint quality. One weakness of MPW is its potentially short metallurgical bond length. Thus, analysis of the effect of process parameters on weld length is important to obtain high-quality joints.

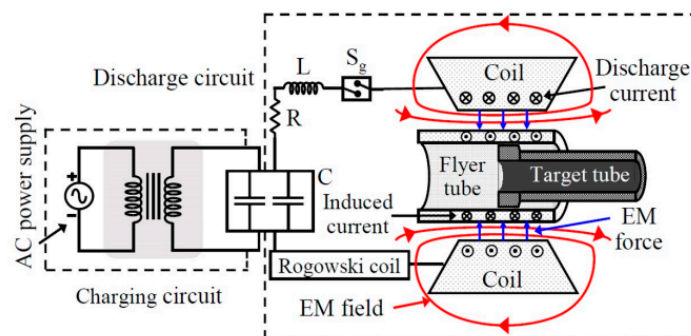


Figure 1. Schematic layout of magnetic pulse welding [12].

Zhang et al. [13] characterized and analyzed the interface structure of an Al/Ta joint, while Geng et al. [14] analyzed the fatigue fracture properties of Al/steel joints using SEM, TEM, and EDS. Recently, Patra et al. [15] performed non-destructive evaluation and investigated the corrosion of Al/steel joints through compositional analysis. Yao et al. [16] discussed the mechanical properties and element diffusion in an additively manufactured 316L to AA5052 MPW joint. This process utilized electromagnetic force, making numerical analysis highly effective for understanding and applying it on site. As a result, researchers have conducted studies using numerical simulations. Shim et al. [17] used a high-accuracy FE model to investigate the characteristics of Al/steel magnetic pulse tubular joints according to discharge time. Bembalge et al. [18] analyzed the effects of gaps between workpieces and of input voltage energy on the mechanical and microstructural properties of joints. Yan et al. [19], utilizing numerical simulations, performed magnetic pulse welding (MPW) with a multiple-seam field-shaper to generate Al/steel joints with uniform circumferential deformation distribution. However, optimizing the MPW process using experimental and numerical methods is challenging due to the need for a large number of trials.

Nowadays, optimization methods are widely used to address problems in welding processes. Notably, response surface methodology (RSM) and the Taguchi method [20,21] are commonly used to determine the relationship between input parameters and output responses, such as joint quality. These methods are effective in minimizing the number of experiments needed for analysis. Shim et al. [1] used RSM to develop a prediction model for burst pressure in dissimilar joints, such as Al/steel and Al/Cu. Ayaz et al. [22] used RSM to investigate the effects of process parameters on the microstructural evolution and mechanical properties of stainless steel and copper joints.

Several evolutionary algorithms have been developed to address optimization problems across a range of scientific and engineering disciplines. These algorithms include the Genetic Algorithm (GA) [23–27], the ant colony optimization algorithm, the bee algorithm, and the Imperialist Competitive Algorithm (ICA) [28–32]. These algorithms establish robust process parameter combinations for achieving superior joint quality. However, the application of evolutionary algorithms to select optimal process parameters in the MPW process has not been explored. Therefore, the objective of this study is to use an evolutionary algorithm to determine the optimal process parameters for achieving maximum weld length. For this, the peak current, gap between workpieces, and frequency were selected as input parameters, while the maximum load and weld length were chosen as output responses. The relationship between the input parameters and the output responses was first examined. Then, a prediction model was developed for application to the evolutionary algorithm. Both ICA and GA were employed as evolutionary algorithms; the determined optimal process parameters were confirmed through verification experiments.

2. Materials and Methods

2.1. Design of the Experiment

The process parameters, such as peak current, gap between workpieces, and frequency, were selected to investigate their effects on the maximum load and weld length. An easy way to estimate the RSM, central composite design (CCD), was employed, and a total of 20 welding conditions were designed to develop the prediction model. The total number of experiments for this study was 20, with three factors ($n = 3$) and five coded levels. The calculation for this number is based on the expression: $(=8: \text{factor points}) + 2n$ ($23 = 6 \text{ axial points}) + 6$ (center points: six replications) [1]. Table 1 lists the design parameters and their corresponding five levels. At the low level (-1), peak current, gap between workpiece, and frequency were set to 350 kA, 0.7 mm, and 17 kHz; at the high level ($+1$), these were set to 450 kA, 1.0 mm, and 20 kHz, respectively, as shown in Table 2.

Table 1. Process parameters and their levels.

Parameter	Unit	Symbol	Level				
			−2	−1	0	1	+2
Peak current	kA	C	316	350	400	450	484
Gap between workpieces	mm	G	0.2	0.4	0.7	1.0	1.2
Frequency	kHz	F	16.0	17	18.5	20	21.0

Table 2. Design of experiment conditions based on CCD.

Run	Input Parameters			Run	Input Parameters		
	C	G	F		C	G	F
1	400	0.7	18.5	11	400	0.7	18.5
2	400	0.7	18.5	12	450	1.0	20.0
3	400	0.2	18.5	13	350	1.0	20.0
4	450	0.4	17.0	14	400	0.7	18.5

Table 2. Cont.

Run	Input Parameters			Run	Input Parameters		
	C	G	F		C	G	F
5	316	0.7	18.5	15	400	0.7	16.0
6	484	0.7	18.5	16	350	0.4	20.0
7	350	0.4	17.0	17	400	0.7	18.5
8	400	1.2	18.5	18	400	0.7	18.5
9	450	1.0	17.0	19	450	0.4	20.0
10	350	1.0	17.0	20	400	0.7	21.0

2.2. Experimental Procedure

This study utilized the magnetic pulse welding system produced by WELMATE Co., Ltd., Cheonan-si, Republic of Korea as shown in Figure 2. This system consists of a pulse power source, a working coil, and a jig/fixture part for welding.

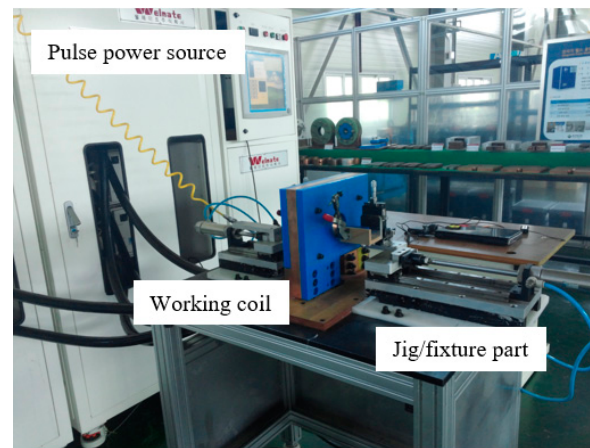


Figure 2. Magnetic pulse welding system.

The pulse power source in this study employed capacitors. Specifically, eight capacitors were connected in parallel, allowing for individual operation. This setup enabled variations in peak current and frequency. Eight triggered switch units were utilized to discharge the capacitors into the coil. The total capacitance of the system was 512 μF , and the charging voltage reached 15 kV. Additionally, to measure the waveform, a Rogowski coil was placed at the junction where the pulse power source and the working coil connect.

The workpieces themselves included an outer workpiece made of an A1070 aluminum tube with a thickness of 0.8 mm. The inner workpiece was made of S45C steel rod. Gaps between workpieces varied depending on the experimental conditions, as detailed in Table 2. The chemical compositions of the workpieces can be found in Table 3.

Table 3. Chemical composition of workpieces (wt.%).

Material	Si	Ga	Ti	Fe	Zn	Al	P	Mn	Cr	C	Fe
A1070	0.07	0.01	0.01	0.20	0.01	Bal	-	-	-	-	-
S45C	0.23	-	-	-	-	-	0.02	0.02	0.08	0.48	Bal

After conducting magnetic pulse welding under various welding conditions, tensile testing and optical microscopy were used to measure the maximum load and weld length, as shown in Figure 3.

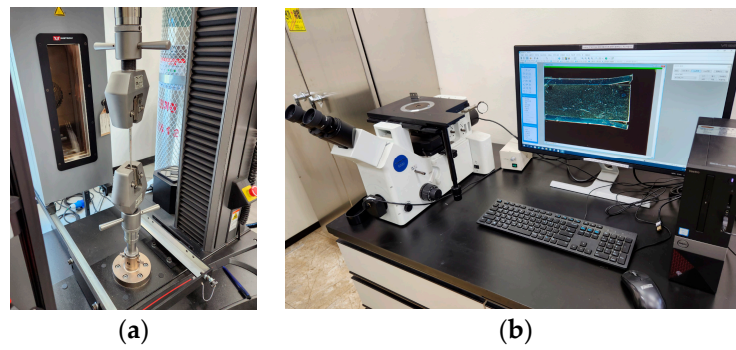
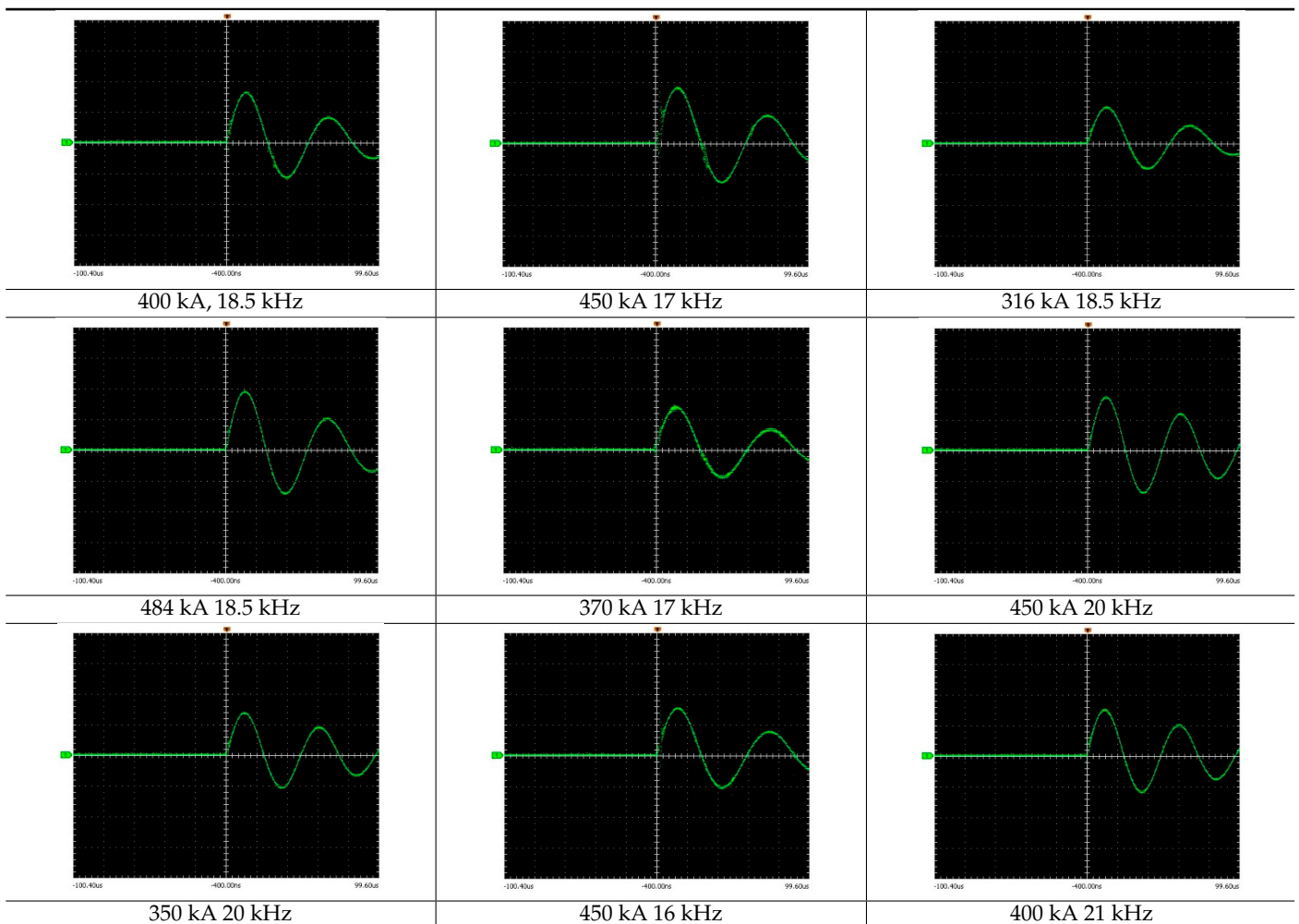


Figure 3. Setup for joint quality evaluation test. (a) Measurement of the maximum load. (b) Observation of weld length.

Table 4 presents waveforms obtained under different welding conditions. This process employed only a quarter of the cycle, precisely until the peak current of the measured waveform [17]. System control allowed for variation of both peak current and frequency of the damped sinusoidal waveform.

Table 4. Discharge waveforms (X: 20 μ s/div, Y: 250 kA/div).



2.3. Results and Discussion

Results of tensile testing and observation of weld length in Tables 5 and 6 show cross sections of joints and maximum loads, respectively.

Table 5. Cross sections of Al/Steel joints.

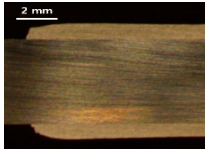
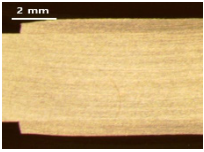
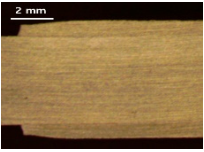
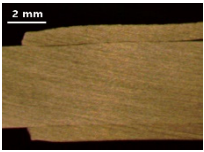
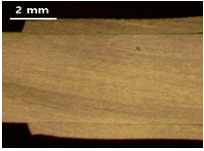
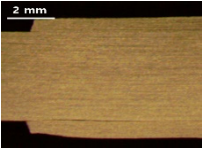
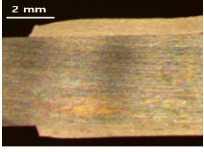
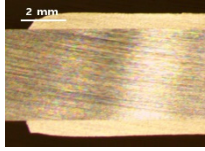
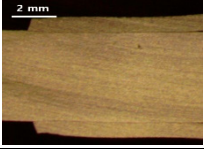
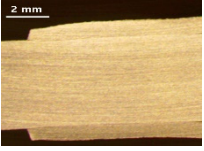
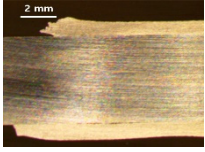
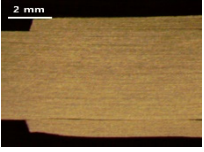
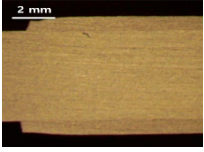
No.	Cross Section	No.	Cross Section	No.	Cross Section	No.	Cross Section
1		6		11		16	
2		7	Separation	12		17	
3	Separation	8	Separation	13		18	
4		9		14		19	
5		10	Separation	15		20	

Table 6. Experimental results.

Trial No.	Input Parameters			Responses	
	C	G	F	Max. Load	Weld Length
1	400	0.7	18.5	1.079	0.27
2	400	0.7	18.5	1.140	0.23
3	400	0.2	18.5	0.043	-
4	450	0.4	17.0	0.785	0.20
5	316	0.7	18.5	0.260	-
6	484	0.7	18.5	1.825	0.54
7	350	0.4	17.0	0.120	-
8	400	1.2	18.5	0.192	-
9	450	1.0	17.0	1.055	0.17
10	350	1.0	17.0	0.042	-
11	400	0.7	18.5	1.143	0.29
12	450	1.0	20.0	1.309	0.50
13	350	1.0	20.0	0.501	0.09
14	400	0.7	18.5	1.069	0.25
15	400	0.7	16.0	0.657	0.10
16	350	0.4	20.0	0.428	0.02
17	400	0.7	18.5	1.067	0.25
18	400	0.7	18.5	1.080	0.27
19	450	0.4	20.0	1.106	0.41
20	400	0.7	21.0	1.467	0.41

2.3.1. Effects of Process Parameters

An analysis of variance (ANOVA) was used to analyze the impacts of parameters on the maximum load and weld length of the joint. Table 7 presents ANOVA results for the mean values of maximum load. The table includes the following symbols: (DF) for degrees of freedom, (Adj SS) for adjusted sum of squares, (Seq SS) for the sequential sum of squares, (Adj MS) for adjusted mean squares, (R-Sq) for coefficient of determination, 'F' for the variance or Fisher ratio of any factor, (Seq SS) for the pure sum of squares of any factor, and 'P' for critical probability. A *p*-value below 0.05 indicates that the model is statistically significant [33]. The results indicate that parameter C has a significant effect on the maximum load, with a contribution of 48.7%. Parameter F follows with a contribution of 10.6%, and parameter G has a contribution of 0.5%. On the other hand, interaction terms such as C × G, G × G, and G × F have negligible effects on the maximum load. The coefficient of determination (R²) for the developed prediction models is 96.02%. MPW is a high-velocity collision welding process.

Table 7. ANOVA table for maximum load.

Source	DF	Adj SS	Adj MS	F-Value	<i>p</i> -Value
Model	9	4.98741	0.55416	101.40	0.000
Linear	3	3.02280	1.00760	184.37	0.000
C	1	2.45984	2.45984	450.09	0.000
G	1	0.02748	0.02748	5.03	0.049
F	1	0.53548	0.53548	97.98	0.000
Square	3	1.93055	0.64352	117.75	0.000
Interaction	3	0.03405	0.01135	2.08	0.167
Error	10	0.05465	0.00547		
Total	19	5.04206			

Based on the ANOVA results, a quadratic polynomial model for maximum load was developed using coded units (i.e., −1, 0, +1). The model can be represented by the following equation:

$$\text{Maximumload} = -10.78 - 0.0152C + 3.08G - 0.521F - 0.000015C^2 - 3.868G^2 - 0.0135F^2 + 0.00342CG + 0.000160CF + 0.0600GF \tag{1}$$

Table 8 presents the ANOVA results for weld length. The results indicate that parameters C and F have significant effects on weld length. Specifically, parameter C has the greatest contribution at 55.1%, followed by parameter F at 17%, and parameter G at 0.2%. Additionally, the interaction terms C × F and C × G influence weld length. The contribution of C × F is 4%, while C × G contributes 0.7%. The developed prediction models have a coefficient of determination (R²) of 95.81%.

Table 8. ANOVA table for weld length.

Source	DF	Adj SS	Adj MS	F-Value	<i>p</i> -Value
Model	9	0.568492	0.063166	140.12	0.000
Linear	3	0.417941	0.139314	309.04	0.000
C	1	0.316236	0.316236	701.52	0.000
G	1	0.001237	0.001237	2.75	0.129
F	1	0.100468	0.100468	222.87	0.000
Square	3	0.122914	0.040971	90.89	0.000
Interaction	3	0.027637	0.009212	20.44	0.000
C × G	1	0.000012	0.000012	0.03	0.871
C × F	1	0.023112	0.023112	51.27	0.000
G × F	1	0.004512	0.004512	10.01	0.010
Error	10	0.004508	0.000451		
Total	19	0.573000			

The ANOVA results led to a quadratic polynomial model for weld length using coded units $(-1, 0, +1)$. The model is represented by the following equation:

$$\text{Weldlength} = 2.07 - 0.00568C + 1.005G - 0.244F - 0.000002C^2 - 1.008G^2 + 0.00133F^2 - 0.00058CG + 0.000583CF + 0.0361GF \quad (2)$$

The peak current and frequency are closely related to the force required for collision with workpieces. If there is insufficient force, the welding may not be of high quality. Figure 4a,c show the effects of peak current and frequency. As the peak current and frequency increase, the maximum load also increases. The gap between workpieces has a role in accelerating the outer workpiece during welding. Notably, the influence of the gap between workpieces was significant; it has optimized values compared to others for achieving the high-quality joint in Figure 4b.

Figure 5 provides a comparison of measured and calculated results obtained using the proposed prediction model for maximum load and weld length. The predicted results agree well with the experimental results. Errors between measured and calculated values were found to be less than 10%, indicating that the proposed prediction model accurately predicted maximum load and weld length.

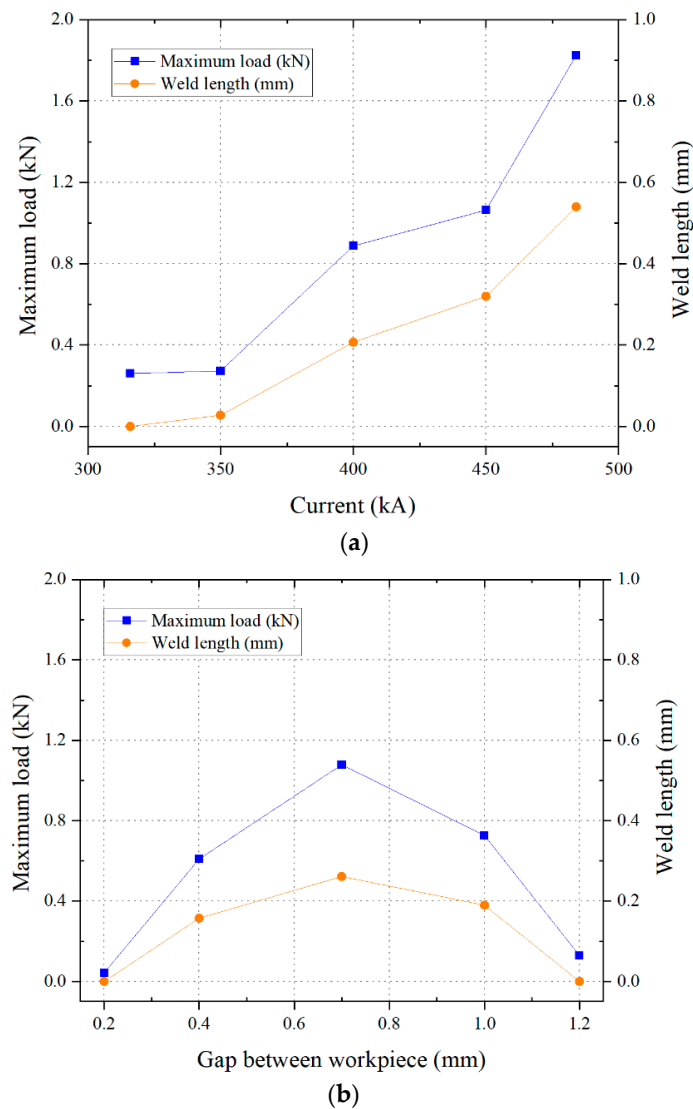


Figure 4. Cont.

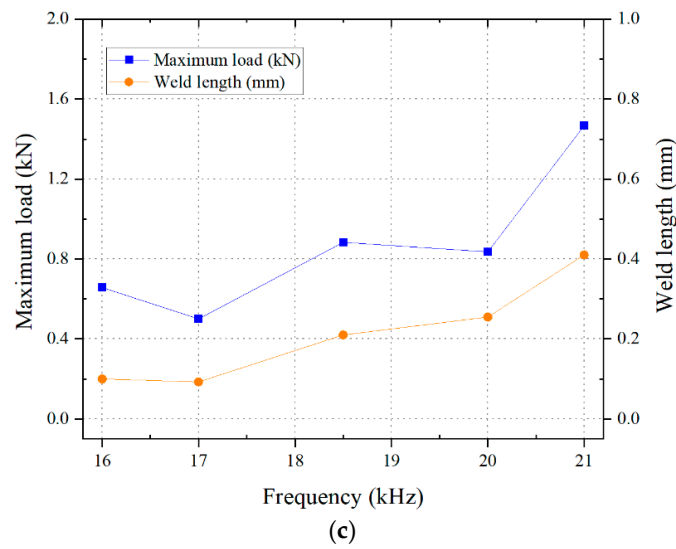


Figure 4. Effects of process parameters on Al/Steel joints. (a) Peak current. (b) Gap between workpieces. (c) Frequency.

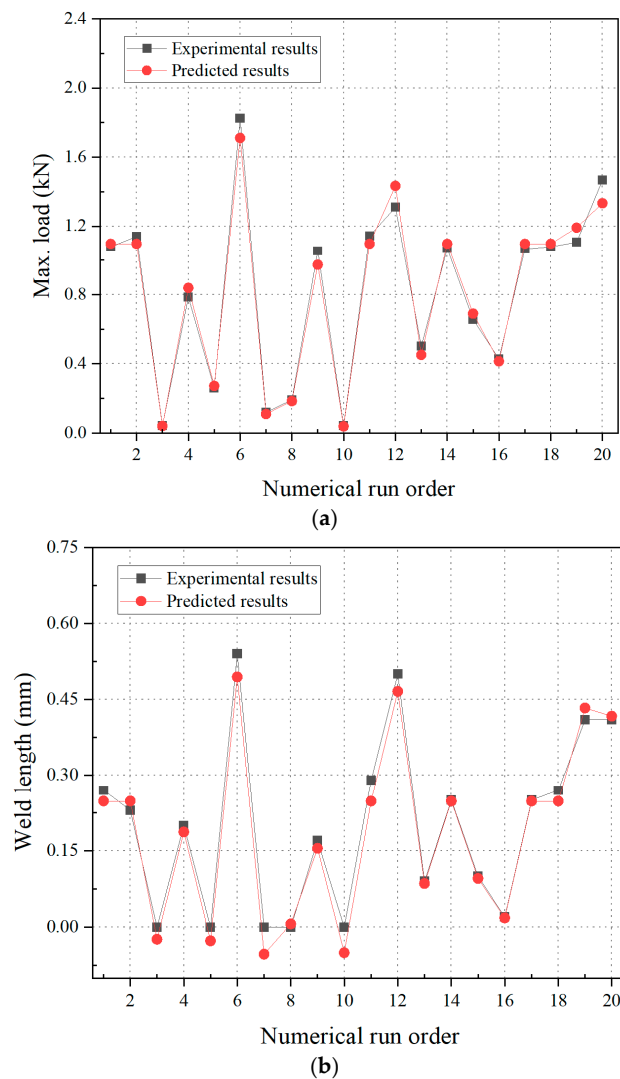


Figure 5. Comparisons between measured and calculated results. (a) Prediction accuracy of developed models for maximum load. (b) Prediction accuracy of developed models for weld length.

2.3.2. Optimization of Process Parameters

(1) Optimization by ICA

The optimization algorithm is a very useful method for finding the proper process parameters for various welding processes. One such algorithm is the Imperialist Competitive Algorithm (ICA), which was developed by Gargari et al. [30]. This is a new meta-heuristic optimization algorithm that incorporates political and social evolution [32]. The algorithm classifies the most powerful nations as imperialists and the rest as colonies. The process consists of five essential stages: empire initialization, assimilation, revolution, competition, and convergence. The first step, empire initialization, entails randomly selecting points from the function to initialize the empires. In an optimization problem with n dimensions, a country is represented by an n -dimensional array [28].

$$\text{Country} = [V_1, V_2, \dots V_n] \tag{3}$$

$$\text{cost} = F(\text{country}) \tag{4}$$

The decision variables in this case are $V_1, V_2, \dots V_n$ and the objective function is represented by F . The second is empire assimilation. The colonies that have a θ degree of deviation and x units move towards the imperialists. This deviation leads to a more thorough exploration of the decision space, as shown in Figure 6 [31]. θ and x are uniformly distributed random numbers. β is a number greater than one, d represents the distance between the imperialists and colonies, and γ is a parameter that determines the extent of deviation from the original direction [28,30–32].

$$x \sim U(0, \beta \times d) \tag{5}$$

$$\theta \sim U(-\gamma, \gamma) \tag{6}$$

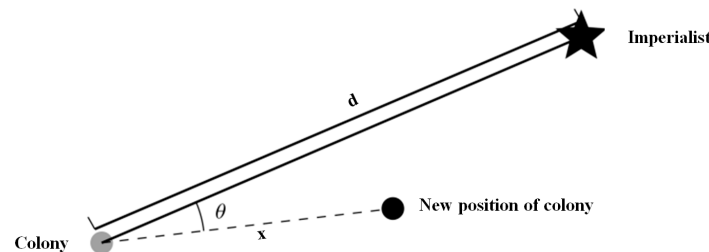


Figure 6. Progression of colonies towards imperialism [31].

As part of the empire-revolution process, certain colonies undergo random repositioning. Following this, in the fourth step, the weakest colony within the weakest empire group is targeted for pillaging by stronger empires as part of the empire competition. This occurrence is determined by the probability proportional to the strength of each imperialist power and the deviation from the average power of the colonies [29].

$$T.C_n = Cost(imperialist_n) + \zeta mean\{Cost(Colonies\ of\ empire_n)\} \tag{7}$$

where $T.C_n$ is the total cost of the n th empire, and ζ is a positive number less than one.

Finally, the competition continues until there is only one imperialist, representing the strongest empire in the search space; this is known as empirical convergence [28–32].

In this study, the effects of varying the number of countries on the maximum load and weld length were investigated. Figure 7 shows the effects of this variation on joint quality. The objective function displayed notable variation when the number of countries was below 80. Increasing the number to 100 marginally enhanced the results. However, further increments in the initial number of countries resulted in decreases in the objective function, although these changes were not significant. Table 9 shows the optimum algorithmic parameters for the ICA model, including the number of countries. These parameters

were determined by trial-and-error. The optimization models were developed using the MATLAB R2018b platform, and the developed prediction models in Section 2.3.1 were embedded into the ICA and optimized.

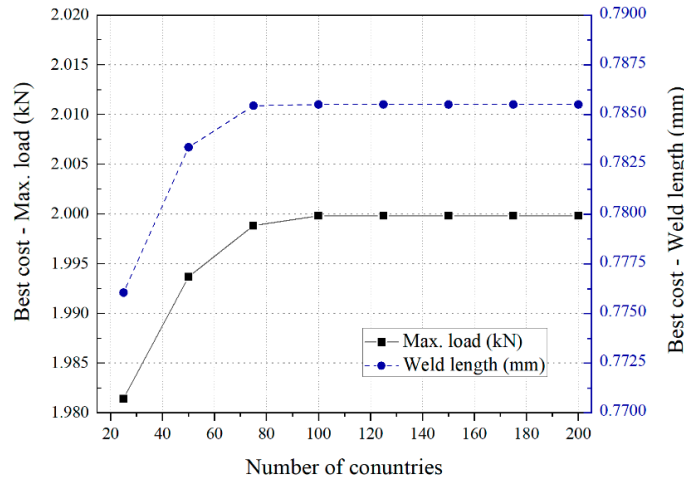


Figure 7. Effect of varying the number of countries on Al/Steel Joint.

Table 9. ICA parameters.

ICA Parameters	Al/Steel MPW
Revolution rate	0.3
Number of Countries	100
Number of Initial Imperialists	6
Number of decades	100
Assimilation Coefficient	1.5
Assimilation Angle Coefficient	0.5
Variable min (C, G, F) (kA, mm, kHz)	(316, 0.2, 16)
Variable max (C, G, F) (kA, mm, kHz)	(484, 1.2, 21)

Figures 8 and 9 show the average and minimum cost, indicating convergence to optimal values. The cost function exhibited a significant decrease in the first five decades. As the iteration proceeded beyond 35 decades, the variation in the cost function became minimal. Specifically, after 42 decades, the maximum load and weld length, which serve as objective functions in this study, were 2.00012 kN and 0.78892 mm, respectively.

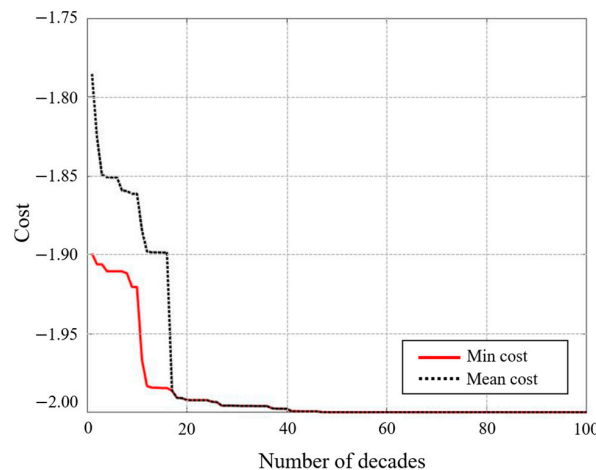


Figure 8. Convergence of maximum load objective function determined by ICA.

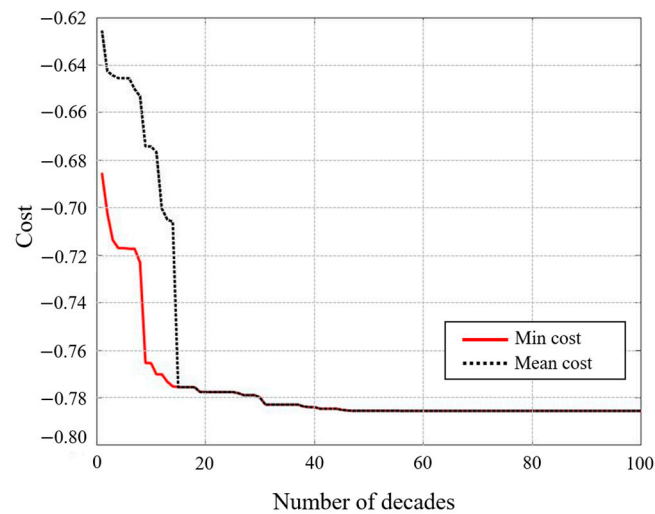


Figure 9. The convergence of the weld length objective function is determined by the ICA.

(2) Optimization by GA

GA, a popular optimization algorithm, is derived from natural evolution processes and originates from Darwin's theory of species evolution. J.H. Holland introduced GA in 1992 [26]. The algorithm utilizes chromosome representations, which are considered points in the solution space. The population's chromosomes are processed through genetic operators to successively replace them. Typically, a GA involves three key steps: selection, crossover, and mutation. First, a random population of chromosomes is created, and the fitness of each chromosome is assessed [24]. If the termination criterion is not met, the process moves on to the following steps. However, if the criterion is met, the best chromosome is returned. The creation of chromosomes continues until a total of n chromosomes are generated [25]. The initial population represents the possible solutions to the optimization problem, and each possible solution is referred to as an individual [23]. A possible solution was formed by the values of the peak current (kA), the gap between workpieces (mm), and the frequency (kHz). The search for the optimum was based on the maximization of the load and weld length, which define the objective function. Table 10 presents the GA parameters that yield the best results: a mutation rate of 0.008, a population size of 100, and a maximum number of generations of 100. Figures 10 and 11 depict the results achieved using the optimal process parameters obtained through GA. These parameters were determined in just 45 generations for the Al/Steel MPW joint. The maximum load and weld length, defining the objective function, were found to be 1.99929 kN and 0.78551 mm, respectively.

Table 10. GA parameters.

GA Parameters	Al/Steel MPW
Population size	100
Number of generations allowed	100
Mutation rate	100
Crossover rate	0.5
Type of crossover	0.5

(3) Comparison of optimization by ICA and GA

A systematic analysis was carried out to evaluate the effectiveness of the proposed algorithms. Both the ICA and GA algorithms were implemented in MATLAB and executed on an INTEL Core-i5 2500M laptop CPU. Table 11 presents a comparison of the optimization results obtained by ICA and GA. It is apparent that ICA slightly outperforms GA in terms of both accuracy and computational time.

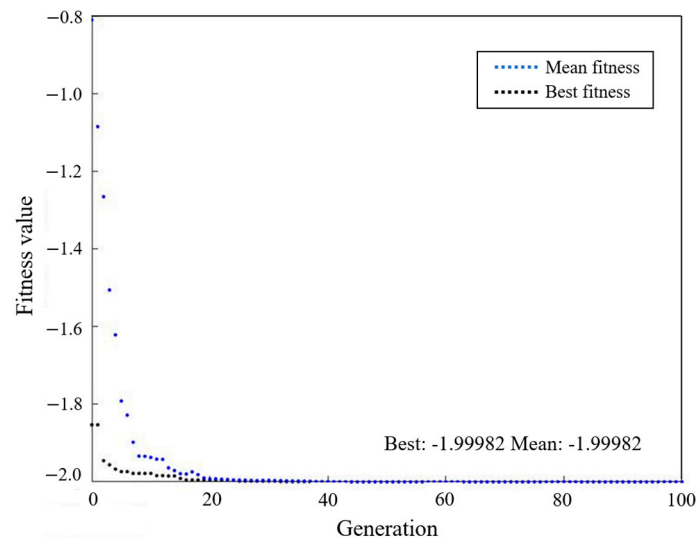


Figure 10. The convergence of the maximum load objective function is determined by GA.

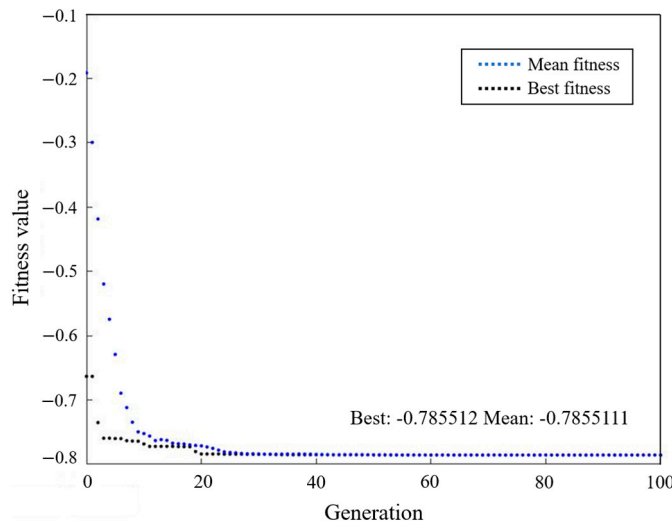


Figure 11. The convergence of the weld length objective function is determined by GA.

Table 11. Comparison between ICA and GA results.

Method	Model	Peak Current (kA)	Gap between Workpieces (mm)	Frequency (kHz)	Cost	CPU Time (s)
ICA	Maximum load (kN)	484	0.77498	21	2.00012	2.9
	Weld length (mm)	483.9	0.73533	21	0.78892	3
GA	Maximum load (kN)	483.9	0.77485	20.9	1.99929	8
	Weld length (mm)	483.9	0.73529	20.9	0.78551	9.4

The optimized process parameters were 484 kA, 0.73 mm, and 21 kHz for peak current, gap between workpieces, and frequency for achieving maximum weld length. Verification of the selected optimal process parameters was performed. The experiment used the optimized process parameters from Table 11 for the joining conditions. After welding, joint qualities were tested according to the maximum values of load and weld length. Figure 12

shows the results of the verification test. The joint at the Al tube was broken, indicating that the strength of the weld joints is greater than the strength of the weaker parent materials, as illustrated in Figure 12a. The maximum load was measured at 2.139 kN. The weld length was measured at 0.8 mm on the joint, as shown in Figure 12b.

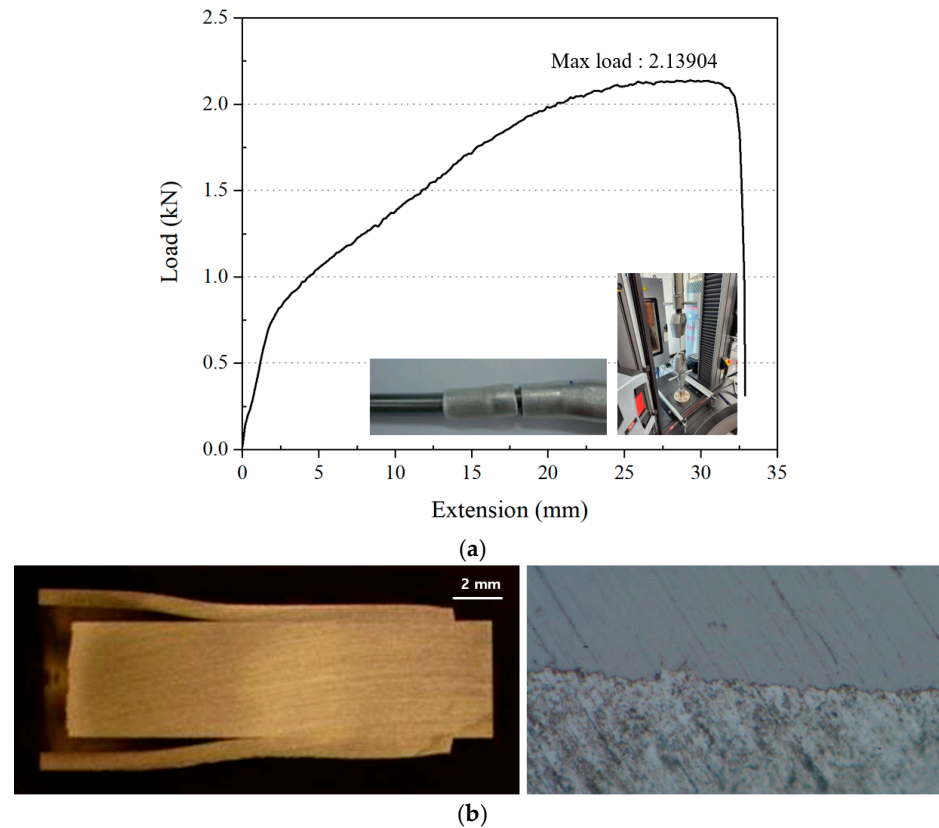


Figure 12. Results of the verification test. (a) Maximum load on Al/Steel joint. (b) Weld length on Al/Steel joint.

3. Conclusions

To improve the maximum load and weld length, this study used ICA and GA as evolutionary algorithms to determine optimal process parameters for Al/Steel MPW joints. The conclusions can be summarized as follows:

- (1) The maximum load and weld length of Al/Steel joints varied under different welding conditions, as determined by CCD. In all cases, the maximum load was measured, but there were five cases in which no weld zone was observed, indicating a separation between Al tube and the steel rod during cutting. From these results, selected MPW process parameters were found to be closely related to joint quality.
- (2) Based on the experimental results, prediction models for maximum load and weld length were developed using RSM. The developed prediction models showed high coefficients of determination (R^2) of 96.02% and 95.81% for maximum load and weld length, respectively. The deviation between actual response values and predicted values was less than 10%, indicating reasonable agreement between the developed prediction models and the experimental results.
- (3) The peak current was discovered to be a crucial factor in enhancing joint quality, specifically in relation to maximum load and weld length, contributing over 48% to the overall quality. Increasing the peak current and frequency improved the quality because the peak current is closely related to the generation of the Lorentz force needed for the collision of workpieces during MPW.
- (4) Optimization was performed using ICA and GA as evolutionary algorithms to select the optimal process parameters. Results from the proposed ICA and GA showed that

ICA performed at a slightly faster rate and yielded higher-quality results than GA. This indicates that the evolutionary algorithm was useful for optimizing the MPW process parameters.

- (5) The optimal process parameters selected using ICA were verified through a verification test. The maximum load and weld length of the Al/Steel MPW joint were measured and found to be 2.139 kN and 0.8 mm, respectively. These results showed good agreement between the ICA-predicted and experimentally-obtained maximum values of load and weld length, confirming that ICA is an effective and useful method for finding optimal process parameters.

Author Contributions: Conceptualization, I.K. and J.S.; Methodology, J.S.; Software, J.S.; Formal analysis, J.S.; Investigation, J.S.; Resources, J.S.; Writing—original draft, J.S.; Writing—review & editing, I.K.; Supervision, I.K. All authors have read and agreed to the published version of the manuscript.

Funding: This research was supported by the Korea Institute of Industrial Technology (KITECH) under one of its major projects, “Development of Smart Welding System Modules with Dynamic Variable Control for Full Penetration Weld (KITECH EH-23-0007).

Data Availability Statement: The data presented in this study are available in this article.

Conflicts of Interest: The authors declare no conflict of interest.

References

1. Shim, J.Y.; Kim, I.S.; Kang, M.J.; Kim, I.J.; Lee, K.J.; Kang, B.Y. Joining of aluminum to steel pipe by magnetic pulse welding. *Mater. Trans.* **2011**, *52*–55, 999–1002. [[CrossRef](#)]
2. Kayode, O.; Akinlabi, E.T. An overview on joining of aluminum and magnesium alloys using friction stir welding (FSW) for automotive lightweight applications. *Mater. Res. Express.* **2019**, *6*–11, 112005. [[CrossRef](#)]
3. Zhao, D.; Liu, F.; Tan, Y.B.; Shi, W.; Xiang, S. Improving the strength-ductility synergy and corrosion resistance of Inconel 718/316L dissimilar laser beam welding joint via post-weld heat treatment. *J. Mater. Res. Technol.* **2023**, *26*, 71–87. [[CrossRef](#)]
4. Chen, L.; Wang, C.; Zhang, X.; Mi, G. Effect of parameters on microstructure and mechanical property of dissimilar joints between 316L stainless steel and GH909 alloy by laser welding. *J. Manuf. Process.* **2021**, *65*, 60. [[CrossRef](#)]
5. Pan, B.; Sun, H.; Shang, S.L.; Banu, M.; Wang, P.C.; Carlson, B.E.; Liu, Z.K.; Li, J. Understanding formation mechanisms of intermetallic compounds in dissimilar Al/steel joint processed by resistance spot welding. *J. Manuf. Process.* **2022**, *83*, 212–222. [[CrossRef](#)]
6. Yang, C.L.; Wu, C.S.; Lv, X.Q. Numerical analysis of mass transfer and material mixing in friction stir welding of aluminum/magnesium alloys. *J. Manuf. Process.* **2018**, *32*, 380–394. [[CrossRef](#)]
7. Bhattacharya, T.K.; Das, H.; Jana, S.S.; Pal, T.K. Numerical and experimental investigation of thermal history, material flow and mechanical properties of friction stir welded aluminium alloy to DHP copper dissimilar joint. *Int. J. Adv. Manuf. Technol.* **2017**, *88*, 847–861. [[CrossRef](#)]
8. Joshania, E.; Beidokhtib, B.; Davodib, A.; Amelzadeh, M. Evaluation of dissimilar 7075 aluminum/AISI 304 stainless steel joints using friction stir welding. *J. Alloys. Metall. Syst.* **2023**, *3*, 100017. [[CrossRef](#)]
9. Kumar, P.; Ghosh, S.K.; De, J.; Barma, S.; Saravanan, b.; Kumar, J. The joining of magnesium and aluminium alloys by inclined arrangement of explosive welding. *Mater. Today Proc.* **2023**, *76*, 536–541. [[CrossRef](#)]
10. Carvalho, G.H.S.F.L.; Mendes, R.; Leal, R.M.; Galvão, I.; Loureiro, A. Effect of the flyer material on the interface phenomena in aluminium and copper explosive welds. *Mater. Des.* **2017**, *122*, 172–183. [[CrossRef](#)]
11. Kapil, A.; Sharma, A. Comprehensive Weldability Criterion for Magnetic Pulse Welding of Dissimilar Materials. *Metals* **2022**, *12*, 1791. [[CrossRef](#)]
12. Faes, K.; Shotri, R.; De, A. Probing Magnetic Pulse Welding of Thin-Walled Tubes. *J. Manuf. Mater. Process.* **2020**, *4*, 118. [[CrossRef](#)]
13. Zhang, W.; Chen, Y.; Xie, J.; Zhang, T.; Wang, S.; Song, X.; Yin, L. Interfacial microstructure of Al/Ta dissimilar joints by magnetic pulse welding. *J. Mater. Res. Technol.* **2023**, *23*, 4167–4172. [[CrossRef](#)]
14. Geng, H.; Sun, L.; Li, G.; Cui, J.; Huang, L.; Xu, Z. Fatigue fracture properties of magnetic pulse welded dissimilar Al-Fe lap joints. *Int. J. Fatigue* **2019**, *121*, 146–154. [[CrossRef](#)]
15. Patra, S.; Singh, G.; Mandal, M.; Chakraborty, R.; Arora, K.S. Non-destructive evaluation and corrosion study of magnetic pulse welded Al and low C steel joints. *Mater. Chem. Phys.* **2023**, *309*, 128315. [[CrossRef](#)]
16. Yao, Y.; Chen, A.; Wang, F.; Jiang, H.; Li, G.; Cui, J. Mechanical properties and joining mechanisms of magnetic pulse welding joints of additively manufactured 316L and conventional AA5052 aluminum alloy. *J. Mater. Res. Technol.* **2023**, *26*, 6146–6161. [[CrossRef](#)]
17. Shim, J.Y.; Kang, B.Y.; Kim, I.S. Characteristics of Al/steel magnetic pulse tubular joint according to discharging time. *J. Mech. Sci. Technol.* **2017**, *31*, 3793–3801. [[CrossRef](#)]

18. Bembalge, O.B.; Singh, B.; Panigrahi, S.K. Magnetic pulse welding of AA6061 and AISI 1020 steel tubes: Numerical and experimental investigation. *J. Manuf. Process.* **2023**, *101*, 128–140. [[CrossRef](#)]
19. Yan, Z.; Xiao, A.; Cui, X.; Guo, Y.; Lin, Y.; Zhang, L.; Zhao, P. Magnetic pulse welding of aluminum to steel tubes using a field-shaper with multiple seams. *J. Manuf. Process.* **2021**, *65*, 214–227. [[CrossRef](#)]
20. Huang, M.L.; Hung, Y.H.; Yang, Z.S. Validation of a method using Taguchi, response surface, neural network, and genetic algorithm. *Measurement* **2016**, *94*, 284–294. [[CrossRef](#)]
21. Muhammad, W.; Husain, W.; Tauqir, A.; Wadood, A. Optimization of friction stir welding parameters of AA2014-T6 alloy using Taguchi statistical approach. *J. Weld. Join.* **2020**, *38–35*, 493–501. [[CrossRef](#)]
22. Ayaz, M.; Khandaei, M.; Vahidshad, Y. Investigating the effect of electromagnetic impact welding parameters on the microstructure evolution and mechanical properties of SS-Cu joint. *Mater. Today Commun.* **2023**, *35*, 105404. [[CrossRef](#)]
23. Liu, B.; Jin, W.; Lu, A.; Liu, K.; Wang, C.; Mi, G. Optimal design for dual laser beam butt welding process parameter using artificial neural networks and genetic algorithm for SUS316L austenitic stainless steel. *Opt. Laser Technol.* **2020**, *125*, 106027. [[CrossRef](#)]
24. Ye, G.Z.; Kang, D.K. Extended Evolutionary Algorithms with Stagnation-Based Extinction Protocol. *Appl. Sci.* **2021**, *11*, 3461. [[CrossRef](#)]
25. Li, Y.B.; Sang, H.B.; Xiong, X.; Li, Y.R. An Improved Adaptive Genetic Algorithm for Two-Dimensional Rectangular Packing Problem. *Appl. Sci.* **2021**, *11*, 413. [[CrossRef](#)]
26. Holland, J.H. *Adaptation in Natural and Artificial Systems*; The University of Michigan Press: Ann Arbor, MI, USA, 1975.
27. Katoch, S.; Chauhan, S.S.; Kumar, V. A review on genetic algorithm: Past, present, and future. *Multimed. Tools Appl.* **2021**, *80*, 8091–8126. [[CrossRef](#)] [[PubMed](#)]
28. Moghari, S.M.H.; Morovati, R.; Moghadas, M.; Araghinejad, S. Optimum Operation of Reservoir Using Two Evolutionary Algorithms: Imperialist Competitive Algorithm (ICA) and Cuckoo Optimization Algorithm (COA). *Water Resour. Manag.* **2015**, *29*, 3749–3769. [[CrossRef](#)]
29. Hemmati, A.; Bahrami, S.; Alaghebandha, M.; Ahmadifard, M. Solving Combined Model Inventory Control with Queuing Theory Approach Using Meta-Heuristic Algorithms. *Middle-East J. Sci. Res.* **2011**, *10–13*, 374–388.
30. Gargari, E.A.; Lucas, C. Imperialist Competitive Algorithm: An Algorithm for Optimization Inspired by Imperialistic Competition. In Proceedings of the 2007 IEEE Congress on Evolutionary Computation, Singapore, 25–28 September 2007; pp. 4661–4667. [[CrossRef](#)]
31. Wang, Z.S.; Lee, J.; Song, C.G.; Kim, S.J. Efficient Chaotic Imperialist Competitive Algorithm with Dropout Strategy for Global Optimization. *Symmetry* **2020**, *12*, 635. [[CrossRef](#)]
32. Luo, J.; Zhou, J.; Jiang, X. A Modification of the Imperialist Competitive Algorithm With Hybrid Methods for Constrained Optimization Problems. *IEEE Access* **2021**, *9*, 161745–161760. [[CrossRef](#)]
33. Madani, T.; Boukraa, M.; Aissani, M.; Chekifi, T.; Ziadi, A.; Zirari, M. Experimental investigation and numerical analysis using Taguchi and ANOVA methods for underwater friction stir welding of aluminium alloy 2017 process improvement. *Int. J. Press. Vessel. Pip.* **2023**, *201*, 104879. [[CrossRef](#)]

Disclaimer/Publisher’s Note: The statements, opinions and data contained in all publications are solely those of the individual author(s) and contributor(s) and not of MDPI and/or the editor(s). MDPI and/or the editor(s) disclaim responsibility for any injury to people or property resulting from any ideas, methods, instructions or products referred to in the content.